Evaluation of antenna radiation characteristics at terahertz frequency band based on an electroopric near-field measurement

Yusuke Tanaka[1], Shintaro Hisatake[1*]
[1]Graduate School of Natural Science and Technology, Gifu University, 501-1193, Yanagido 1-1, Gifu, Japan
*Corresponding author: hisatake@gifu-u.ac.jp

Abstract – The near-field of a horn antenna at 288 GHz was measured based on the non-polarimetric EO frequency down conversion technique and self-heterodyne technique. The measured near-field was converted to the far-field and compared with the simulated characteristic to examine the fidelity of our results. The measured radiation characteristics roughly agreed with the simulated results.

Keywords – Terahertz; Antenna measurement; EO sensing; Near-field;

1. Introduction

In the terahertz (THz: 0.1 - 10 THz) band, many applications have been considered in these days such as wireless communication [1], non-destructive inspection [2], etc. In these applications, antennas are one of the important components to determine the system performance, therefore many antennas operating in the THz frequency band have been studied [3, 4]. In order to optimize the performance of the applications, it is necessary to accurately determine the antenna radiation pattern. However, the evaluation method has not been established in the THz wave band.

We have developed an electrooptic (EO) sensing system, which is based on a non-polarimetric frequency down conversion technique and self-heterodyne techniques, to reveal the spatial and temporal evolution of freely propagating continuous THz waves [5, 6]. This system enabled us to measure near-field of the THz wave radiated from the antenna.

In this paper, we visualize the near-field of the THz wave (288 GHz) and calculate the far-field radiation pattern from the measured near-field. We also compare the far-field with the simulated results and evaluate the quality of our measurement.

2. System configuration

Figure 1 shows the experimental set up for the antenna near-field measurement using an electrooptic (EO) probe. The size of the EO crystal is $1\times1\times1$ mm^3. The frequencies of the LDs were set to be f_1 and f_2 and combined to generate a beat note at a frequency of 288 GHz ($\lambda = 1.04$ mm) for the RF signal. The optical beat signal was converted to the THz signal by uni-traveling-carrier photodiode (UTC-PD). The generated THz wave was emitted from a horn antenna. The optical

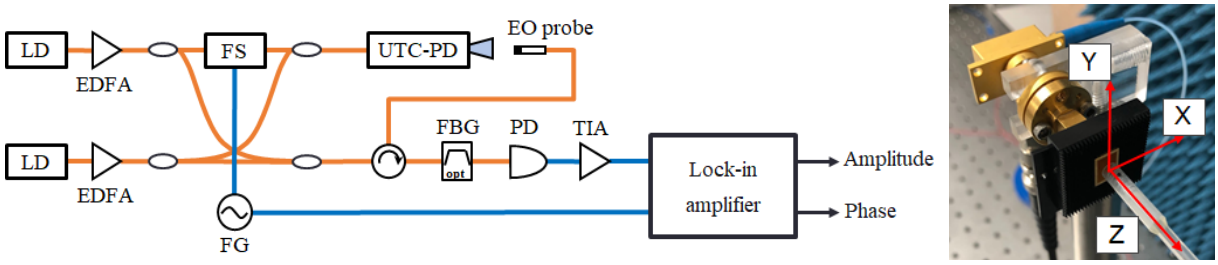

Figure 1. Experimental setup for the antenna near-field measurement. The system is based on a non-polarimetric EO frequency down conversion technique and self-heterodyne technique. UTC-PD: Uni-traveling-carrier photodiode, FS: frequency shifter, LD: laser diode, EDFA: Erbium doped optical fiber amplifier, TIA: transimpedance amplifier, FG: function generator, FGB: fiber bragg grating.

beat signal was also sent to the EO probe to sense the amplitude and phase of the THz wave. The EO probe was moved to map the near-field distribution on the antenna surface. As shown in Figure 1, the antenna was surrounded by an absorber.

3. Experimental result and discussion

Figure 3 shows the amplitude and phase distribution. The measured surface was at Z=2 mm from the antenna surface. The EO probe was moved by 0.1 mm pitch. The time constant of the lock-in detection was 30 ms. The maximum signal-to-ratio (SNR) was about 37 dB at the center of the surface.

Figure 4 shows the far-field patterns. The simulation was conducted using CST studio suite. The measured near-field was converted to the far-field. Measured far-fields roughly agreed with the simulated results. However, the measured results have asymmetric pattern in both of E-plane and H-plane. Also, the position of the sidelobes did not coincide with the simulated values.

Table 1 summarizes the radiation pattern characteristics. The deviation between the simulated and measured values for the 3-dB beam width were 0.3 deg. and 0.7 deg. for the H-plane and E-plane, respectively. The deviation for the sidelobe position was about 1 deg. and 2.5 deg. for the first and second sidelobe in the E-plane, respectively. We believe that those discrepancies were due to the EO probe characteristics. It is presumed that the characteristics of the probe are determined by the size of the EO crystal with respect to the wavelength. The sensitivity characteristics also depend on the incident direction of the signal to the EO crystal. The probe correction should be conducted to improve the measurement accuracy.

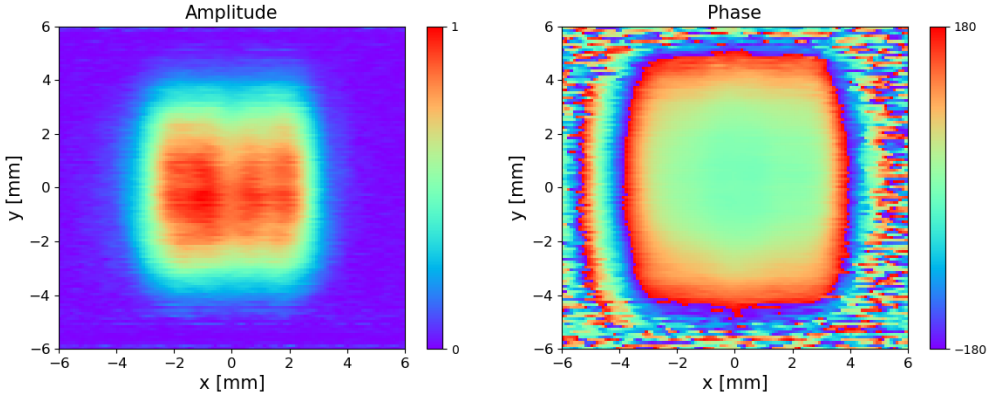

Figure 3. The measured amplitude and phase distribution. The amplitude is normalized to the maximum value.

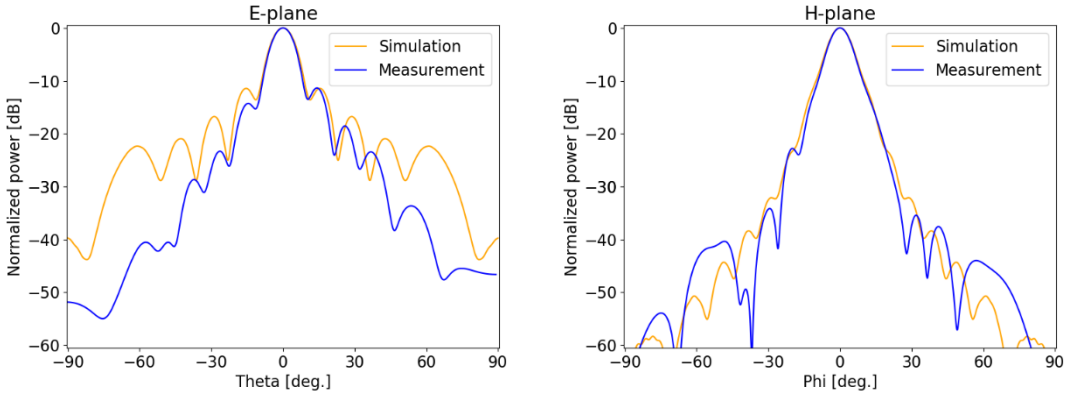

Figure 4. Measured and simulated far-field pattern. The measured near-field was converted to the far-field.

Table 1. Characteristics of the radiation pattern.

			Measurement	Simulation
H-plane 3dB beam width [deg.]			9.4	9.7
E-plane 3dB beam width [deg.]			9.5	10.2
E-plane	$+1^{st}$ sidelobe	Position [deg.]	14.22	15.42
		Main lobe ratio [dB]	-11.36	-11.43
	-1^{st} sidelobe	Position [deg.]	-14.55	-15.42
		Main lobe ratio [dB]	-14.28	-11.43
	$+2^{nd}$ sidelobe	Position [deg.]	25.94	28.76
		Main lobe ratio [dB]	-18.54	-16.74
	-2^{nd} sidelobe	Position [deg.]	-26.41	-28.76
		Main lobe ratio [dB]	-23.30	-16.74

4. Conclusion

We demonstrated far-field characterization of a horn antenna in the THz frequency band based on the near-field EO sensing. The measured radiation characteristics roughly agreed with the simulated results. Small discrepancy between the measurement and the simulation is due to the probe characteristics at this frequency band. The probe correction may be conducted to improve the fidelity of the measurements.

Acknowledgements

This research is partially supported by funding from Horizon 2020, the European Union's Framework Program for Research and Innovation, under grant agreement No. 814523. ThoR has also received funding from the National Institute of Information and Communications Technology in Japan.

References

[1] Oshima N, Hashimoto K, Horikawa D, Suzuki S, Asada M. Wireless data transmission of 30 Gbps at a 500-GHz range using resonant-tunneling-diode terahertz oscillator. 2016 IEEE MTT-S International Microwave Symposium (IMS) May 22-27, 2016, San Francisco, CA, USA.

[2] Zhang H, Sfarra S, Saluja K, Peeters J, Fleuret J, Duan Y, et al. Non-destructive Investigation of Paintings on Canvas by Continuous Wave Terahertz Imaging and Flash Thermography. J Nondestruct Eval. 2017; 36:34.

[3] Deng X, Li Y, Liu C, Wu W, Xiong Y. 340 GHz on-chip 3-D antenna with 10 dBi gain and 80% radiation efficiency. IEEE Trans. Terahertz Sci. Technol, 2015; vol.5, pp.619-627.

[4] Li L, Li Y, Yeo T, Mosig J, Martin O A. Broadband and High-Gain Metamaterial Microstrip Antenna. Appl. Phys. Lett. 2010; vol.96, 164101.

[5] Hisatake S, Nagatsuma T. Nonpolarimetric Technique for Homodyne-type Electrooptic Field Detection. Appl. Phys. Express 2012; vol. 5, 012701.

[6] Hisatake S, Nguyen Pham H H, Nagatsuma T. Visualization of the spatial temporal evolution of continuous electromagnetic waves in the terahertz range base d on photonics technology. Optica, 2014; vol.1, no.6, pp.365-371.

[7] Hisatake S, Kitahara G, Ajito K, Fukada Y, Yoshimoto N, Nagatsuma T. Phase-Sensitive Terahertz Self-Heterodyne System Based on Photodiode and Low-Temperature-Grown GaAs Photoconductor at 1.55 μm. IEEE Sensors Journal. 2013; vol. 13, pp.31-36.